NATIONAL ADVISORY COMMITTEE FOR AERONAUTICS

TECHNICAL NOTE 3594

EFFECT OF TRANSVERSE BODY FORCE ON CHANNEL FLOW WITH SMALL HEAT ADDITION

By Simon Ostrach and Franklin K. Moore

Lewis Flight Propulsion Laboratory
Cleveland, Ohio

Washington
February 1956

NATIONAL ADVISORY COMMITTEE FOR AERONAUTICS

TECHNICAL NOTE 3594

EFFECT OF TRANSVERSE BODY FORCE ON CHANNEL FLOW WITH SMALL HEAT ADDITION

By Simon Ostrach and Franklin K. Moore

SUMMARY

The steady, compressible, inviscid channel flow to which heat is added at a cross-sectional plane and which is also subject to a transverse body force is analyzed. The prime parameters governing the flow are a dimensionless heat parameter and the Mach and Froude numbers. Solutions which are qualitatively similar are obtained for the cases in which either the Mach number is small or the Froude number is large. If the heat is added uniformly over the plane, the streamlines are displaced in the direction of the body force, and downstream of the heat addition the flow is found to be a shear flow. If the heat addition is concentrated near the center of the cross-sectional plane, a strong vortex motion appears downstream in addition to the shear flow. In the first part of the analysis, the through-flow Mach number is considered small. Subsequently, the alternate assumption of large Froude number is made. For large Froude numbers it is found that an increase in Mach number to unity increases the magnitude of the body-force effects.

The configuration studied can be considered to be an idealization of, for example, the flow in a ram jet mounted at the tip of a whirling helicopter rotor blade. The effects of the transverse body force are important in this example. Actually, even if the Froude number is large, the vortex motion due to any nonuniformity of heat addition may be quite vigorous.

INTRODUCTION

It is well known that the motion of a fluid in which there are density variations is altered by the action of body forces on the fluid. Until recently, such buoyancy effects have been negligible in practical applications, because both the density variations and the body forces were relatively small. However, considerations of present-day propulsion systems with their associated large heat additions, rapidly rotating components, or their operation in sudden maneuvers at high speeds

suggest a reevaluation of these effects. Of prime importance in this respect is the effect of the body forces on the internal aerodynamics of such propulsion systems or their components. The influence of the body forces has been studied for channel flows with uniform heat addition and with the body force parallel to the direction of motion (see ref. 1, e.g.). The flow with heat addition in pipe bends, through rotor-tip combustors of helicopters, or through ram jets in abrupt maneuvers represents configurations of interest in which, on the other hand, the body force is transverse to the flow direction.

Configurations of the latter type will be considered herein. More specifically, in the present analysis a steady uniform (in velocity and temperature) flow in a channel subject to a transverse body force is assumed perturbed by a steady small addition of heat at a cross-sectional plane (fig. 1). The fluid is considered to be inviscid. The neglect of viscosity is in contrast to the analysis of reference 1. The reason for this difference can be explained as follows:

Important body-force effects appear in regions of large temperature gradients transverse to the body-force direction. In internal natural-convection flow problems (ref. 1, e.g.), the largest temperature gradients occur in the viscous heat-conducting layers of fluid next to the channel walls; accordingly, a parameter (Grashof number) comparing viscous and body-force effects governs the solutions of these problems. In the present problem, the important temperature gradient is not associated with viscous wall effects, but, rather, with the addition of heat at a flame front or combustion zone. Therefore, the fluid may be considered inviscid in this problem; and the Froude number, which compares inertia forces and body forces, and not the Grashof number is of chief importance. In addition, of course, a parameter specifying rate of heat addition to the fluid and the Mach number are also of significance.

If heat is added uniformly over the cross section (fig. 2(a)), the sudden reduction of density at $x = 0$ (for small through Mach number) would be expected to cause the streamlines to have a tendency to rise in the vicinity of the heat addition. Perhaps the most interesting effects may be expected when heat is added over only part of the cross section, as in figure 2(b). Then, the difference in buoyancy between the flow near the center and the flow near the edges of the channel would be expected to result in the formation of vortices with axes alined with the through flow.

With a view to studying these flow patterns, solutions are sought for the perturbation equations further simplified by the assumption of small Mach number or, alternatively, of large Froude number.

The cooperation of Mr. Julius P. Peline on part of the detail development of the analysis reported herein is gratefully acknowledged.

DIFFERENTIAL EQUATIONS AND BOUNDARY CONDITIONS

Basic Equations

The differential equations governing the steady flow with heat addition of a compressible, inviscid, nonconducting fluid which is subject to a body force are, in rectangular Cartesian tensor notation,

$$\frac{\partial}{\partial X_j}(\rho U_j) = 0 \tag{1a}$$

$$\rho U_j \frac{\partial U_i}{\partial X_j} = \rho f_i - \frac{\partial P}{\partial X_i} \tag{1b}$$

$$\rho c_v U_j \frac{\partial T}{\partial X_j} = Q - P \frac{\partial U_j}{\partial X_j} \tag{1c}$$

$$\frac{P}{\rho} = RT \tag{1d}$$

(A complete list of the symbols used herein is presented in the appendix.) Equations (1a) to (1c) express, respectively, the conservation of mass, momentum, and energy; equation (1d) is the state equation. The more familiar notation U,V,W and X,Y,Z instead of U_1,U_2,U_3 and X_1,X_2,X_3 will be used in the remainder of this report.

Boundary Conditions

Particular consideration is given to the configuration illustrated in figure 1: Far upstream, there is a flow with uniform velocity and temperature in a straight channel, so that

$$U(-\infty,Y,Z) = U_\infty \text{ (a constant)} \tag{2a}$$

$$V(-\infty,Y,Z) = W(-\infty,Y,Z) = 0 \tag{2b}$$

$$T(-\infty,Y,Z) = T_\infty \text{ (a constant)} \tag{2c}$$

The channel has a uniform rectangular cross section, so that

$$V(X,0,Z) = V(X,H,Z) = 0 \tag{3a}$$

$$W(X,Y,0) = W(X,Y,L) = 0 \tag{3b}$$

The fluid is subject to a transverse body force f_2 acting in the direction of positive Y. Thus, f_1 and f_3 are defined to be zero, and f_2 is a negative quantity if the body force acts in the direction illustrated in figure 1. The action of the body force leads to pressure and density gradients in an equilibrium state. This equilibrium will be disturbed by the addition of heat to the fluid.

Thus two specific problems are treated herein according to the specified distribution of heat addition. If heat is added uniformly (fig. 2(a)) over the cross section at $X = 0$, the problem is two dimensional in X and Y. A three-dimensional problem will also be treated, in which the rate of heat addition at $X = 0$ varies with the coordinate Z, which is transverse to the direction of body force (see fig. 2(b)).

However, the analysis will be carried forward as far as possible with an arbitrary function to represent heat addition.

Linearization of Equations

In the present analysis, a perturbation procedure will be employed. Accordingly, the actual rate of heat addition per unit volume Q at $X = 0$ is included in the dimensionless quantity

$$\varepsilon q(X,Y,Z) \equiv \frac{QH}{\rho_\infty U_\infty c_p T_\infty} \tag{4}$$

where the function q is of unit order and ε is a small parameter. As a consequence of the small rate of heat addition, the flow is assumed to be disturbed only slightly from the uniform conditions prevailing far upstream (eqs. (2)). The disturbances are assumed to be of the order ε, and the following definitions are made:

$$\left.\begin{aligned} U = U_\infty\left(1 + \varepsilon \frac{\rho_r}{\rho_\infty} u\right),\ V = \varepsilon U_\infty \frac{\rho_r}{\rho_\infty} v,\ W = \varepsilon U_\infty \frac{\rho_r}{\rho_\infty} w \\ T = T_\infty(1 + \varepsilon\tau),\ P = P_\infty + \varepsilon P_r \sigma,\ \rho = \rho_\infty + \varepsilon \rho_r X \end{aligned}\right\} \tag{5}$$

where ρ_r is a constant reference density. Also, dimensionless coordinates are defined as

$$x,y,z \equiv X/H,\ Y/H,\ Z/H \tag{6}$$

respectively.

Substituting equations (5) and (6) into equations (1) yields, to zero order in ε,

$$\left.\begin{aligned} \frac{d\rho_\infty}{dy} &= -\frac{\gamma M_\infty^2}{Fr^2}\rho_\infty \\ P_\infty(y) &= RT\rho_\infty(y) \end{aligned}\right\} \tag{7}$$

so that

$$\rho_\infty = \rho_r \exp(-\gamma M_\infty^2 y/Fr^2)$$

and

$$P_\infty = P_r \exp(-\gamma M_\infty^2 y/Fr^2)$$

These expressions involve the Froude and Mach numbers defined by

$$\left.\begin{aligned} Fr &\equiv U_\infty/\sqrt{(-f_2)H} \\ M_\infty &\equiv U_\infty/\sqrt{\gamma RT_\infty} \end{aligned}\right\} \tag{8}$$

Clearly, equations (7) express the conditions of static equilibrium of density and pressure with body force, if no heat is added. In such a case, the presence of a uniform through velocity U_∞ would not affect this equilibrium.

The following equations to the first order in ε result upon elimination of σ, τ, and χ from the equations obtained by combining (1), (5) and (6):

$$u_{xz} - w_{xx} = 0 \tag{9a}$$

$$u_{xy} - v_{xx} + \lambda(u_x + v_y + w_z) = 0 \tag{9b}$$

$$(1 - M_\infty^2)u_x + v_y + w_z + \lambda(\gamma - 1)M_\infty^2 v = q \tag{9c}$$

where $\lambda = 1/Fr^2$ and, hence, represents essentially the ratio of body to inertia forces.

Definition of a Potential

In order to reduce the number of variables of equations (9), a function ψ is defined such that

$$\psi_{xx} \equiv \lambda(u_x + v_y + w_z) \tag{10}$$

From equations (1a), (5), and (10) it may be shown that the function ψ is related to the perturbation in density:

$$\psi_x = -\lambda\chi$$

Then, in view of equations (2) and (10), the Cauchy-Riemann conditions may be extracted from equations (9) in the form

$$\left.\begin{aligned} u_z - w_x &= 0 \\ u_y - (v - \psi)_x &= 0 \\ w_y - (v - \psi)_z &= 0 \end{aligned}\right\} \tag{11}$$

Accordingly, a potential φ may be defined so that

$$\left.\begin{aligned} u &\equiv \varphi_x \\ v - \psi &\equiv \varphi_y \\ w &\equiv \varphi_z \end{aligned}\right\} \tag{12}$$

Equations (9c) and (10) to (12) yield

$$\nabla^2\varphi - M_\infty^2\varphi_{xx} + (\gamma - 1)\lambda M_\infty^2\varphi_y = q - \psi_y - (\gamma - 1)\lambda M_\infty^2\psi \tag{13a}$$

$$\psi_{xx} - \lambda\psi_y = \lambda\nabla^2\varphi \tag{13b}$$

Equations (2), (5), (6), (10), and (12) yield the boundary conditions to which equations (13) are subject:

$$\varphi(-\infty,y,z) = \psi(-\infty,y,z) = 0 \tag{14a}$$

$$\varphi_y(x,0,z) + \psi(x,0,z) = \varphi_y(x,1,z) + \psi(x,1,z) = 0 \tag{14b}$$

$$\varphi_z(x,y,0) = \varphi_z\left(x,y,\frac{L}{H}\right) = 0 \tag{14c}$$

Hereinafter, the heat addition will be assumed to occur abruptly at $x = 0$. That is,

$$q \equiv \delta(x)q^*(y,z) \tag{15}$$

where $\delta(x)$ is the Dirac delta function.

SOLUTIONS OF SPECIAL PROBLEMS

Small Mach Number

Equations (13), while linear, are not especially simple. Therefore, results will be obtained under further simplifying assumptions If the Mach number is sufficiently small so that $M_\infty^2 \ll 1$ and the Froude number is of unit order, then, in place of equations (13),

$$\psi = \lambda \int_{-\infty}^{x} dx \int_{-\infty}^{x} \delta(x)q^*dx = \lambda x\, 1(x)q^* \tag{16a}$$

$$\nabla^2\varphi = \delta(x)q^* - \lambda x\, 1(x)q_y^* \tag{16b}$$

where $1(x)$ is the unit step function.

Quite evidently, equations (13) may also be simplified by the assumption of small (but nonvanishing) λ. This approach will be discussed in the subsequent section, Large Froude Number.

Reduction of potential problem to familiar forms. - In order to obtain a more familiar problem of potential theory, equation (16b) may be solved in two parts, defining

$$\varphi = \varphi_1 + \varphi_2 \tag{17a}$$

where

$$\nabla^2\varphi_1 = q = \delta(x)q^* \tag{17b}$$

and

$$\nabla^2\varphi_2 = -\lambda \int_{-\infty}^{x} dx \int_{-\infty}^{x} q_y dx = -\lambda x\, l(x) q_y^* \tag{17c}$$

A function which is a particular integral of equation (17c) for $x > 0$ is

$$\varphi_3 = -\lambda x\, l(x) h(y,z) \tag{18a}$$

where $h(y,z)$ satisfies Poisson's equation

$$h_{yy} + h_{zz} = q_y^* \tag{18b}$$

but is otherwise unspecified, as yet. Then, if the definition

$$\varphi_2 = \varphi_3 + \varphi_4 \tag{19}$$

is made, substituting equations (18) into equation (17c) yields

$$\nabla^2\varphi_4 = \lambda \delta(x) h(y,z) \tag{20}$$

Except precisely at $x = 0$, φ_1 and φ_4 satisfy Laplace's equation. Solutions of Laplace's equation, valid for $x < 0$ and $x > 0$, are denoted by superscripts $-$ and $+$, respectively. Integrating equations (17b) and (20) across the discontinuity in the plane $x = 0$ yields the compatibility conditions

$$\left(\varphi_{1x}^{+} - \varphi_{1x}^{-}\right)_{x=0} = q^* \tag{21a}$$

$$\left(\varphi_{4x}^{+} - \varphi_{4x}^{-}\right)_{x=0} = \lambda h \tag{21b}$$

In addition to equations (21), the boundary conditions (eqs. (14)) must be satisfied.

Thus, after the singular solution (eq. (18a)) is extracted, the remaining differential equations are simply Laplace's equation (applied independently for $x > 0$ and $x < 0$) subject to the jump conditions of equations (21) and Poisson's equation (18b) in two dimensions.

Fourier series solution for $q^* = q^*(z)$. - The foregoing equations may readily be solved by Fourier analysis, if q^* is assumed to be a function only of z (fig. 2), representable as

$$q^*(z) = \sum_{n=0}^{\infty} Q_n \cos \pi n\alpha z \tag{22}$$

where $\alpha = H/L$. A solution of Laplace's equation which also satisfies equations (14a), (14c), and (21a) is

$$\varphi_1^+ = Q_0 x - \sum_{n=1}^{\infty} \frac{Q_n}{2\pi n\alpha} e^{-\pi n\alpha x} \cos \pi n\alpha z \tag{23a}$$

$$\varphi_1^- = - \sum_{n=1}^{\infty} \frac{Q_n}{2\pi n\alpha} e^{\pi n\alpha x} \cos \pi n\alpha z \tag{23b}$$

Because $q_y^* = 0$, it is permissible to take

$$h(y,z) = \sum_{0}^{\infty} Q_n \frac{\sinh \pi n\alpha\left(y - \frac{1}{2}\right)}{\pi n\alpha \cosh \frac{\pi n\alpha}{2}} \cos \pi n\alpha z \tag{24}$$

as the proper solution of equation (18b). In view of the definition of ψ (eq. (16a)) and of equation (22), this choice provides that φ_3 (eq. (18a)) satisfies equation (14b). Also, equation (14a) remains satisfied.

The function φ_4 must be found so that it is consistent with equation (21b). Also, of course, φ_4 must satisfy equations (14a) and (14c) and together with φ_3 must satisfy equation (14b).

Being antisymmetric about the plane $y = 1/2$, the y-dependence of $h(y,z)$ in equation (24) is represented by the Fourier series in order that the boundary conditions can be satisfied. Thus,

$$Q_n \frac{\sinh \pi n\alpha\left(y - \frac{1}{2}\right)}{\pi n\alpha \cosh \frac{\pi n\alpha}{2}} = \sum_{m=0}^{\infty} B_{mn} \cos m\pi y \tag{25a}$$

where, by Fourier's theorem,

$$\left.\begin{aligned} B_{mn} &= 0 \qquad (m \text{ zero or even}) \\ &= -\frac{4}{\pi^2\left[m^2 + \alpha^2 n^2\right]} Q_n \qquad (m \text{ odd}) \end{aligned}\right\} \tag{25b}$$

Then, equation (24) becomes

$$h = \sum_{m=0}^{\infty}\sum_{n=0}^{\infty} B_{mn} \cos m\pi y \cos \pi n\alpha z \tag{26}$$

and, from equation (21b), the proper equation for φ_4 must be

$$\varphi_4^{\pm} = -\frac{\lambda}{2\pi}\sum_{m=0}^{\infty}\sum_{n=0}^{\infty} \frac{B_{mn} e^{\mp\pi x\sqrt{m^2+\alpha^2n^2}}}{\sqrt{m^2 + \alpha^2 n^2}} \cos m\pi y \cos \pi n\alpha z \tag{27}$$

satisfying equation (21b).

To recapitulate equations (17a), (18a), (19), (23), (24), and (27), the result for φ is

$$\varphi^{\pm} = x\,1(x)\left[Q_0 - \lambda\sum_{n=0}^{\infty} Q_n \frac{\sinh \pi n\alpha\left(y - \frac{1}{2}\right)}{\pi n\alpha \cosh \frac{\pi n\alpha}{2}} \cos \pi n\alpha z\right] - \sum_{n=1}^{\infty} \frac{Q_n}{2\pi n\alpha} e^{\mp\pi n\alpha x} \cos \pi n\alpha z$$

$$- \frac{\lambda}{2\pi}\sum_{m=0}^{\infty}\sum_{n=0}^{\infty} \frac{B_{mn}}{\sqrt{m^2 + \alpha^2 n^2}} e^{\mp\pi x\sqrt{m^2+\alpha^2n^2}} \cos m\pi y \cos \pi n\alpha z \tag{28}$$

Result for uniform heat addition. - In the instance of uniform heat addition (fig. 2(a)), $q^*(z) = Q_0$ from equation (22), with all other Q_n being zero. Then, incorporating equation (25b) and using L'Hospital's rule yield for equation (28):

$$\varphi^{\pm} = Q_0\left\{x\,1(x)\left[1 - \lambda\left(y - \frac{1}{2}\right)\right] + \frac{2\lambda}{\pi^3}\sum_{j=0}^{\infty} \frac{e^{\mp(2j+1)\pi x}}{(2j+1)^3} \cos(2j+1)\pi y\right\} \tag{29a}$$

Also, from equation (16a),

$$\psi = \lambda x \, 1(x) Q_0 \tag{29b}$$

The velocity components, from equations (12), are

$$u^{\pm} = Q_0 \left\{ 1(x) \left[1 - \lambda \left(y - \frac{1}{2} \right) \right] \mp \frac{2\lambda}{\pi^2} \sum_{j=0}^{\infty} \frac{e^{\mp(2j+1)\pi x}}{(2j+1)^2} \cos(2j+1)\pi y \right\} \tag{30a}$$

$$v^{\pm} = - Q_0 \frac{2\lambda}{\pi^2} \sum_{j=0}^{\infty} \frac{e^{\mp(2j+1)\pi x}}{(2j+1)^2} \sin(2j+1)\pi y \tag{30b}$$

The result for vertical velocity (eq. (30b)) indicates that fluid streamlines are displaced downward as they traverse the section where heat is added in proportion to the amount of heat added Q_0 and the Froude number (through λ). Such a streamline is shown in side view in figure 3(a). Inasmuch as equation (30b) is symmetrical in x, one-half the displacement occurs upstream of the heat addition. The total displacement of a streamline near the center of the channel ($y = 1/2$) is approximately, from equations (4), (5), (7), and (30b),

$$\int_{-\infty}^{\infty} \frac{V}{U_\infty} \, dx = - \frac{1}{8} \varepsilon Q_0 \lambda = - \frac{1}{8} \lambda \int_{-\infty}^{+\infty} \frac{QH \, dx}{\rho_\infty U_\infty c_p T_\infty} \tag{31}$$

where the integral is, essentially, the total rate of heat addition per unit area.

This displacement occurs in a distance of the order of H and is in a downward sense. Figure 3(a) shows that downward displacement is, in fact, consistent with a buoyant force acting at $x = 0$. The streamline curvature which is negative for $x < 0$ and positive for $x > 0$ suffers an abrupt upward increase at $x = 0$. Of course, the restraint imposed by the walls at $y = 0,1$ determines the particular streamline pattern to accompany the upward buoyant acceleration at $x = 0$.

The result for the dimensionless through velocity U/U_∞, from equations (5) and (30a), is indicated in figure 3(b). Far upstream (station 1) the flow has a dimensionless uniform velocity 1. Far downstream (station 4), the average dimensionless velocity is higher by εQ_0

because of the heat addition.[1] Because of the buoyancy effect, the velocity profile has a uniform shear of such a magnitude that the dimensionless velocity difference between the bottom and top of the channel is $\varepsilon Q_0 \lambda$. For large distances downstream, this is the dominant effect of Froude number. The sense of the shear is such that the through flow is more rapid in the constricted flow in the lower part of the channel (cf. figs. 3(a) and (b)), and less in the expanded flow at the top. This result is in accord with the usual behavior of one-dimensional low-speed flow in a channel of varying area.

In view of equation (21a), the actual velocity jump at $x = 0$ must be independent of y and z. This requirement is met by the potential flow described by the series terms of equations (30). Evaluated at $x = 0$, these terms yield the dashed-line profiles in figure 3, which are parallel and differ by the constant εQ_0, between stations 2 and 3.

The potential-flow terms attenuate exponentially in distances of the order of H, both upstream and downstream from the zone of heat addition. At large distances, the most persistent of the series terms is the first one, yielding contributions to u and v proportional to $\exp[\mp\pi x][\cos \pi y]$ and $\exp[\mp\pi x][\sin \pi y]$, respectively.

Result for cosine-wave heat addition. - For the problem of cosine-wave heat addition (fig. 2(b)),

$$q^*(z) = \frac{1}{2}\tilde{Q}(1 - \cos 2\pi\alpha z) \tag{32}$$

Thus, from equation (22), $Q_0 = \frac{1}{2}\tilde{Q}$, $Q_2 = -\frac{1}{2}\tilde{Q}$, and, from equation (28),

$$\varphi^{\pm} = \frac{1}{2}\tilde{Q}\left\{x\,1(x)\left[1 - \lambda\left(y - \frac{1}{2} - \frac{\sinh 2\pi\alpha\left(y - \frac{1}{2}\right)}{2\pi\alpha \cosh \pi\alpha}\cos 2\pi\alpha z\right)\right] + \frac{1}{4\pi\alpha}e^{\mp 2\pi\alpha x}\cos 2\pi\alpha z\right\}$$
$$- \frac{\lambda}{2\pi}\sum_{m=0}^{\infty}\frac{B_{m0}}{m}e^{\mp\pi m x}\cos m\pi y - \frac{\lambda}{2\pi}\cos 2\pi\alpha z \sum_{m=0}^{\infty}\frac{B_{m2}}{\sqrt{m^2 + (2\alpha)^2}}e^{\mp\pi x\sqrt{4\alpha^2 + m^2}}\cos m\pi y \tag{33a}$$

[1]The factor ρ_r/ρ_∞ is omitted here and in similar expressions in this section on small Mach numbers, because its value is unity to consistent order in Mach number (see eqs. immediately following eq. (7)).

and, from equation (16a),

$$\psi = \lambda x \, 1(x) \frac{\tilde{Q}}{2} (1 - \cos 2\pi\alpha z) \tag{33b}$$

Again, part of the solution involves potential functions, attenuating at distances of the order of H and L upstream and downstream of the station $x = 0$, where heat is added.

On an average across the channel, streamlines are displaced downward, as in the previous case of constant heat addition. The velocity components which dominate for larger x are, from equations (33) and (12),

$$u = \frac{1}{2} \tilde{Q} \left\{ 1 - \lambda \left[y - \frac{1}{2} - \frac{\sinh 2\pi\alpha \left(y - \frac{1}{2} \right)}{2\pi\alpha \cosh \pi\alpha} \cos 2\pi\alpha z \right] \right\} \tag{34a}$$

$$v = -\frac{1}{2} \tilde{Q} \lambda x \left[1 - \frac{\cosh 2\pi\alpha \left(y - \frac{1}{2} \right)}{\cosh \pi\alpha} \right] \cos 2\pi\alpha z \tag{34b}$$

$$w = -\frac{1}{2} \tilde{Q} \lambda x \frac{\sinh 2\pi\alpha \left(y - \frac{1}{2} \right)}{\cosh \pi\alpha} \sin 2\pi\alpha z \tag{34c}$$

Equations (34) represent an incompressible vortex motion, satisfying the simple continuity equation $u_x + v_y + w_z = 0$, and having the dimensionless components of vorticity

$$\Omega_x \equiv w_y - v_z = -\pi \tilde{Q} x \lambda \alpha \sin 2\pi\alpha z \tag{35a}$$

$$\Omega_y \equiv u_z - w_x = 0 \tag{35b}$$

$$\Omega_z \equiv v_x - u_y = \frac{\tilde{Q}\lambda}{2} (1 - \cos 2\pi\alpha z) \tag{35c}$$

Equation (34a) defines the part of the profile of u (fig. 4) which corresponds to the shear flow (eq. (31)) occurring in the case of uniform heat addition (station 4, fig. 3). This portion of the profile does not vary with x. In fact, from equations (35b) and (35c) the related vorticity components Ω_y and Ω_z are also constant with x. Of course, equations (34b), (34c), and (35a) are valid only for moderate x, inasmuch as the present analysis is restricted to small perturbations. Since, physically, the vortices must be finite even far downstream, the conditions far from the plane of heat addition must be determined from a more complete analysis.

In the present three-dimensional case, there is a tendency to form strong vortices with axes alined with the flow. These vortices are indicated by the streamline pattern for a cross section shown in figure 5. The axial vorticity Ω_x increases linearly with x, as equation (35a) evidences; the amount of circulation in each half of the cross section is found to be equal to $\varepsilon\lambda\tilde{Q}U_\infty Hx$.

Another view of the vortex motion is obtained by tracing the vortex filaments of the flow. Each filament lies in a plane of constant y ($\Omega_y = 0$, from eq. (35b)) and is horseshoe-shaped, with the open end downstream. The vortex filaments lying in the plane $y = 1/2$ are shown as dotted lines in figure 5. If the horseshoes are spaced equally in x (this is required by the fact that Ω_z is independent of x, from eq. (35c)), the number of filaments passing through a cross section apparently is directly proportional to x. Accordingly, Ω_x must increase linearly with x.[2] These results are, of course, for M_∞ essentially equal to zero. The effects of Mach number will be determined in the subsequent section.

Large Froude Number

As has been stated, simplification of equations (13) can also be obtained by assuming that the Froude number is large so that $\lambda = \frac{1}{Fr^2}$ rather than the Mach number is small relative to unity. Therefore, expanding φ and ψ in a Maclaurin series in λ as

$$\left.\begin{aligned} \varphi &= \varphi^{(0)} + \lambda\varphi^{(1)} + \cdots \\ \psi &= \psi^{(0)} + \lambda\psi^{(1)} + \cdots \end{aligned}\right\} \tag{36}$$

yields to zero order in λ

$$\nabla^2\varphi^{(0)} - M_\infty^2\varphi_{xx}^{(0)} = q - \psi_y^{(0)} \tag{37}$$

---

[2]The vortex system illustrated in fig. 5 suggests a comparison with the system of bound vortices of a low-aspect-ratio wing, with a leading edge at $x = 0$ and with a span of L. The sense of the vortices in the present problem corresponds to a wing with negative lift distribution, and this is consistent with the downward inclination of the flow which has previously been discussed as occurring in the vicinity of the heat addition.

$$\psi_{xx}^{(0)} = 0 \tag{38}$$

and to first order in λ

$$\nabla^2\varphi^{(1)} - M_\infty^2\varphi_{xx}^{(1)} = -\left[\psi_y^{(1)} + (\gamma - 1)M_\infty^2\left(\varphi_y^{(0)} + \psi^{(0)}\right)\right] \tag{39}$$

$$\psi_{xx}^{(1)} = \nabla^2\varphi^{(0)} + \psi_y^{(0)} \tag{40}$$

The boundary conditions for equations (37) to (40) are

$$\varphi^{(i)}(-\infty,y,z) = \psi^{(i)}(-\infty,y,z) = 0 \tag{41a}$$

$$\varphi_y^{(i)}(x,0,z) + \psi^{(i)}(x,0,z) = \varphi_y^{(i)}(x,1,z) + \psi^{(i)}(x,1,z) = 0 \tag{41b}$$

$$\varphi_z^{(i)}(x,y,0) = \varphi_z^{(i)}\left(x,y,\frac{L}{H}\right) = 0 \tag{41c}$$

where i is 0 and 1 for the zero- and first-order equations, respectively. In view of equations (36), the zero-order solutions describe the flow with heat addition and no body force, and the first-order solutions represent the contributions due to the action of the body forces. Thus, in order to find the effects of a transverse body force on the flow, the first-order solutions must be determined. However, in the case of the small Mach number previously treated, the body-force effects are evident from the zero-order (in Mach number) solutions. Thus, for small Mach numbers, the body-force effects can be of the same order of magnitude as the effects of heat addition; whereas, for small λ, the body-force effects must be small relative to the heat-addition effects. The solutions of the previous section are, therefore, perhaps more meaningful, but the present section serves to show how the Mach number affects the flow.

Fourier series solution. - From the boundary conditions and equation (38), it is evident that

$$\psi^{(0)} \equiv 0 \tag{42}$$

This fact together with the transformations

$$\xi = x$$

$$\eta = \beta y$$

$$\zeta = \beta z$$

$$\beta = \sqrt{1 - M_\infty^2}$$

for $M_\infty^2 < 1$ reduces equation (37) to a Poisson equation like equation (17b), except that the independent variables are ξ, η, and ζ and the coefficient $1/\beta^2$ appears on the right side of the equation. For heat addition of the type specified by equations (15) and (22), $\varphi^{(0)}$ satisfies Laplace's equation everywhere except precisely at $x = 0$. Thus, $\varphi^{(0)}$ must also satisfy the compatibility condition

$$\left(\varphi_\xi^{(0)+} - \varphi_\xi^{(0)-}\right)_{\xi=0} = q^*/\beta^2$$

The zero-order solution then is similar to equations (23) and in the x,y,z system can be written as

$$\varphi^{(0)+} = \frac{Q_0 x}{\beta^2} - \sum_{n=1}^{\infty} \frac{Q_n}{2\pi n\alpha\beta} e^{-\frac{\pi n\alpha x}{\beta}} \cos \pi n\alpha z \qquad (43a)$$

$$\varphi^{(0)-} = -\sum_{n=1}^{\infty} \frac{Q_n}{2\pi n\alpha\beta} e^{\frac{\pi n\alpha x}{\beta}} \cos \pi n\alpha z \qquad (43b)$$

This solution is independent of y as expected, since to the zero order the effects of the body force are not included. Recall that the restriction $M_\infty^2 < 1$ has already been imposed. Therefore, the factors β and β^2 in the denominators of equations (43) and others in this section should cause no concern.

In order to solve the first-order system, substitute equations (37) into equation (40), integrate, and apply the boundary conditions to yield

$$\psi^{(1)} = M_\infty^2 \varphi^{(0)} + x\, l(x) q^* \qquad (44)$$

3593

Since q^* is independent of y, $\psi^{(1)}$ is also, and equation (39) becomes

$$\nabla^2\varphi^{(1)} - M_\infty^2\varphi_{xx}^{(1)} = 0 \tag{45}$$

From equations (41b) and (44), the solution for $\varphi^{(1)}$ involves the removal of the singularity at $x = 0$, just as in the small Mach number case previously discussed. Therefore, in a manner similar to the previous method (eqs. (41b) and (44)), let

$$\varphi^{(1)} = \bar{\varphi} - M_\infty^2 y\varphi^{(0)} - x\,l(x)h(y,z) \tag{46}$$

where h is given by equation (24). Combining equations (41), (45), and (46) yields

$$\beta^2\bar{\varphi}_{xx} + \bar{\varphi}_{yy} + \bar{\varphi}_{zz} = \delta(x)\left[M_\infty^2 yq^* + \beta^2 h(y,z)\right] \tag{47}$$

$$\bar{\varphi}(-\infty,y,z) = 0 \tag{48a}$$

$$\bar{\varphi}_y(x,0,z) = \bar{\varphi}_y(x,l,z) = 0 \tag{48b}$$

$$\bar{\varphi}_z(x,y,0) = \bar{\varphi}_z\left(x,y,\frac{L}{H}\right) = 0 \tag{48c}$$

Applying equation (24) and the previously given transformation to the ξ,η,ζ coordinate system to equation (47) yields

$$\nabla^{*2}\bar{\varphi} = \frac{\delta(\xi)}{\beta^2}\sum_{n=0}^{\infty}\sum_{m=0}^{\infty} C_{mn}\cos\frac{\pi m\eta}{\beta}\cos\frac{\pi n\alpha\zeta}{\beta} \tag{49}$$

where ∇^{*2} denotes the Laplacian operator for the independent variables ξ, η, and ζ and where the Fourier series representation

$$\sum_{m=0}^{\infty} C_{mn}\cos\frac{\pi m\eta}{\beta} = Q_n\left[\frac{M_\infty^2\eta}{\beta} + \frac{\beta^2\sinh\pi n\alpha\left(\frac{\eta}{\beta} - \frac{1}{2}\right)}{\pi n\alpha\cosh\frac{\pi n\alpha}{2}}\right]$$

with

$$C_{mn} = \frac{Q_n M_\infty^2}{2} \qquad (m = 0) \qquad (50a)$$

$$= 0 \qquad (m \text{ even}) \qquad (50b)$$

$$= -\frac{4Q_n}{\pi^2}\left[\frac{M_\infty^2}{m^2} + \frac{\beta^2}{(m^2 + \alpha^2 n^2)}\right] \qquad (m \text{ odd}) \qquad (50c)$$

is used in order that the boundary conditions on $\bar{\varphi}$ can be satisfied. The solution $\bar{\varphi}$ once again satisfies Laplace's equation except precisely at $\xi = 0$ so that the following compatibility condition must also be satisfied:

$$\left(\bar{\varphi}_\xi^+ - \bar{\varphi}_\xi^-\right)_{\xi=0} = \frac{1}{\beta^2}\sum_{n=0}^{\infty}\sum_{m=0}^{\infty} C_{mn}\cos\frac{\pi m\eta}{\beta}\cos\frac{\pi n\alpha\zeta}{\beta}$$

Hence, in the x,y,z system

$$\bar{\varphi}^{\pm} = \frac{1}{\beta^2}\left(x\,1(x)C_{00} - \frac{\beta}{2\pi}\sum_{m+n=1}^{\infty}\sum \frac{C_{mn}e^{\mp\frac{\pi x}{\beta}\sqrt{m^2+(\alpha n)^2}}}{\sqrt{m^2 + (\alpha n)^2}}\cos \pi my \cos \pi n\alpha z\right) \qquad (51)$$

Thus, from equations (36), (43), (46), (24), and (51) the function φ for large Froude numbers is to the first order in λ

$$\varphi^{\pm} = (1 - \lambda M_\infty^2 y)\left(\frac{x\,1(x)Q_0}{\beta^2} - \sum_{n=1}^{\infty}\frac{Q_n}{2\pi n\alpha\beta}e^{\mp\frac{\pi n\alpha x}{\beta}}\cos \pi n\alpha z\right)$$

$$+ \lambda\left[\frac{x\,1(x)C_{00}}{\beta^2} - \left(\frac{1}{2\pi\beta}\sum_{m+n=1}^{\infty}\sum \frac{C_{mn}}{\sqrt{m^2 + (\alpha n)^2}}e^{\mp\frac{\pi x}{\beta}\sqrt{m^2+(\alpha n)^2}}\right)\right.$$

$$\left.\left(\cos m\pi y \cos \pi n\alpha z\right) - x\,1(x)\sum_{n=0}^{\infty}\frac{Q_n}{\pi n\alpha}\frac{\sinh \pi n\alpha\left(y - \frac{1}{2}\right)}{\cosh\frac{\pi n\alpha}{2}}\cos \pi n\alpha z\right] \qquad (52)$$

For zero Mach number, this solution reduces to that given for small Mach numbers by equation (28).

Result for uniform heat addition. - For uniform heat addition, as shown in figure 2(a), equation (22) becomes $q^*(z) = Q_0$ with all other Q_n being zero. Then using equation (50) and applying L'Hospital's rule to equation (52) yield

$$\varphi^{\pm} = Q_0\left[\frac{x\,1(x)}{\beta^2}\left(1 - \lambda y + \frac{\lambda}{2}\right) + \frac{2\lambda}{\pi^3\beta}\sum_{j=0}^{\infty}\frac{e^{\mp\frac{\pi(2j+1)x}{\beta}}}{(2j+1)^3}\cos(2j+1)\pi y\right] \tag{53}$$

Also, from equations (36), (42), and (44)

$$\psi = \frac{\lambda Q_0 x\,1(x)}{\beta^2} \tag{54}$$

From equations (12), (53), and (54) the velocity components are

$$u^{\pm} = \frac{Q_0}{\beta^2}\left[1(x)\left(1 - \lambda y + \frac{\lambda}{2}\right) \mp \frac{2\lambda}{\pi^2}\sum_{j=0}^{\infty}\frac{e^{\mp\frac{\pi(2j+1)x}{\beta}}}{(2j+1)^2}\cos(2j+1)\pi y\right] \tag{55a}$$

$$v^{\pm} = -\frac{2\lambda Q_0}{\pi^2\beta}\sum_{j=0}^{\infty}\frac{e^{\mp\frac{\pi(2j+1)x}{\beta}}}{(2j+1)^2}\sin(2j+1)\pi y \tag{55b}$$

Except for the factor $1/\beta$ in the coefficient and exponent of equation (55b), this equation and equation (30b) are identical. With increasing Mach number, then, and large Froude number, the total downward displacement of a streamline remains the same as in the small Mach number case; however, the axial distance over which the displacement occurs is decreased.

The jump across $x = 0$ in the dimensionless increment of through velocity u is, from equation (55a), equal to Q_0/β^2; thus, the Mach number increases the jump. The series term in equation (55a), which, as has been pointed out, corresponds to a potential, also is increased with Mach number but dies out because of Mach number effects at shorter distances on either side of the plane $x = 0$.

The component of u

$$u = -\frac{Q_0\lambda}{\beta^2}\left(y - \frac{1}{2}\right)$$

represents a shear flow downstream of the heat addition and, again, is increased by Mach number.

Result for cosine-wave heat addition. - In order to find the effects of nonuniform heat addition in a plane transverse to the through flow, a cosine-wave heat-source distribution is assumed (fig. 2(b)), and $q^*(z)$ is given by equation (32). For this case, equation (52) becomes

$$\varphi^{\pm} = \frac{\tilde{Q}}{2}\left(\frac{x\,1(x)}{\beta^2}\left\{1 - \lambda\left[y - \frac{1}{2} - \frac{\beta^2 \sinh 2\pi\alpha\left(y - \frac{1}{2}\right)}{2\pi\alpha \cosh \pi\alpha}\cos 2\pi\alpha z\right]\right\} + \frac{\left(1 - \lambda M_\infty^2 y\right)}{4\pi\alpha\beta} e^{\mp \frac{2\pi\alpha x}{\beta}} \cos 2\pi\alpha z\right) - \frac{\lambda}{2\pi}\sum_{m=1}^{\infty} \frac{C_{m0}}{m} e^{\mp \frac{\pi m x}{\beta}} \cos m\pi y$$

$$- \frac{\lambda}{2\pi}\cos 2\pi\alpha z \sum_{m=0}^{\infty} \frac{C_{m2}}{\sqrt{m^2 + (2\alpha)^2}} e^{\mp \frac{\pi x}{\beta}\sqrt{m^2+(2\alpha)^2}} \cos m\pi y \qquad (56)$$

and, from equations (36), (42), and (44),

$$\psi = \frac{\lambda\tilde{Q}}{2}\left[\frac{x\,1(x)}{\beta^2}\left(1 - \beta^2 \cos 2\pi\alpha z\right) + \frac{M_\infty^2 e^{\mp \frac{2\pi\alpha x}{\beta}}}{4\pi\alpha\beta}\cos 2\pi\alpha z\right] \qquad (57)$$

The velocity components, determined from equations (12), (56), and (57), once again are composed of potential flows which vanish at distances of the order of H and L upstream and downstream of the heat-addition zone and the following components which persist for large x:

$$u = \frac{\tilde{Q}}{2}\left\{\frac{1}{\beta^2} - \lambda\left[\frac{y - \frac{1}{2}}{\beta^2} - \frac{\sinh 2\pi\alpha\left(y - \frac{1}{2}\right)}{2\pi\alpha \cosh \pi\alpha}\cos 2\pi\alpha z\right]\right\} \qquad (58a)$$

$$v = -\frac{\tilde{Q}\lambda x}{2}\left[1 - \frac{\cosh 2\pi\alpha\left(y - \frac{1}{2}\right)}{\cosh \pi\alpha}\right]\cos 2\pi\alpha z \qquad (58b)$$

$$w = -\frac{\tilde{Q}\lambda x}{2}\frac{\sinh 2\pi\alpha\left(y - \frac{1}{2}\right)}{\cosh \pi\alpha}\sin 2\pi\alpha z \tag{58c}$$

The v and w components are identical to those found in the previous section (eqs. (34b) and (34c)) and are independent of Mach number. The only effects of Mach number are apparent in equation (58a), which defines a shear flow in this case which corresponds to that determined for uniform heat addition. The Mach number, however, increases the average (over the channel width) shear flow as compared with that for small Mach number (see eq. (34a)). The jump in axial velocity is also increased with Mach number. Equations (58) satisfy the simple continuity equation $u_x + v_y + w_z = 0$ and represent a vortex motion having components of vorticity

$$\Omega_x = -\pi\tilde{Q}x\alpha\lambda \sin 2\pi\alpha z \tag{59a}$$

$$\Omega_y = 0 \tag{59b}$$

$$\Omega_z = \frac{\tilde{Q}\lambda}{2}\left[\frac{1}{\beta^2} - \cos 2\pi\alpha z\right] \tag{59c}$$

The x-component is identical to that given by equation (35a) for small Mach numbers, but the z-component is decreased by the Mach number. Therefore, although the cross-sectional streamline pattern is unchanged by Mach number (see fig. 5), the slope of the vortex filaments Ω_z/Ω_x is infinite at the walls, as shown on the following sketch, instead of

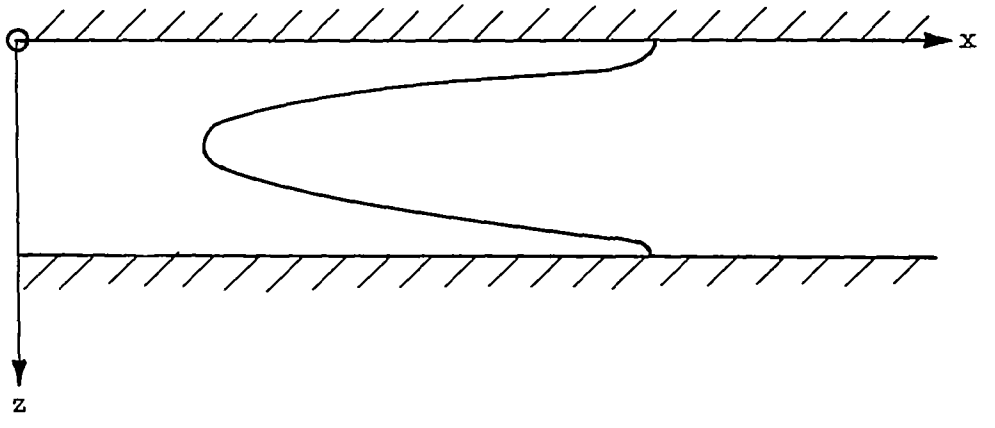

extending indefinitely downstream, as in figure 5.

Helicopter Rotor-Tip Ram-Jet Combustors

The solutions of the previous sections are all linearly dependent on λ. Therefore, the order of magnitude of λ will be determined in a practical problem. For this determination, consideration is given to the rotor-tip combustors of helicopter ram jets. It must, of course, be realized that the configuration analyzed herein is only an idealization of an actual unit of this kind. Thus,

$$\lambda = -\left(\frac{U_T}{U_\infty}\right)^2 \frac{H}{r}$$

where U_T is the tip speed, r is the rotor radius, and U_∞, of course, is the speed of the gas at which combustion is to take place. It is clear that the ratio H/r will be small in a practical case ($H/r = 1/16$ would be a possible value), whereas U_T/U_∞ will be large, assuming that the flow at the inlet must be diffused to low velocity in the combustor (a diffusion ratio of $U_T/U_\infty = 4$ would be possible). Thus, values of λ of unit order magnitude are not unreasonable. Actually, even if λ is small, the analysis indicates that vortex motions can occur with nonuniform heat addition.

For the case of uniform heat addition, the order of magnitude of the nonuniformity of the resulting flow can be estimated from the ratio of the velocity difference between the bottom and top of the channel D to the jump in velocity across the plane of heat addition ΔU. This ratio $D/\Delta U$ is just equal to λ. For nonuniform heat addition, the ratio $\Gamma/(2H + L)\overline{\Delta U}$ will yield an order of magnitude for the flow nonuniformity where Γ is the circulation in half the channel cross section and the bar over ΔU indicates that this is the average over z. Thus

$$\frac{\Gamma}{(2H + L)\overline{\Delta U}} = \lambda \frac{x}{(1 + L/2H)}$$

Therefore, in both cases the nonuniformity in the flow evidently will be of the same order as λ and hence can be appreciable as is demonstrated herein for helicopter ram-jet tip combustors.

SUMMARY OF RESULTS

An analysis of the steady, compressible, inviscid channel flow to which heat is added at a cross-sectional plane and which is subject to a transverse body force showed how the flow depends on the Mach and Froude numbers and a dimensionless heat parameter. Solutions were

obtained for uniform or nonuniform heat addition at a cross-sectional plane under the simplifying assumption of either small Mach number or of large Froude number. For small Mach numbers and uniform heat addition, the flow was displaced in the direction of the body force with the velocity profile being one of uniform shear. Nonuniform heat addition in the cross-sectional plane in this case lead to the superposition of strong vortex motions on the shear flow.

The solutions for large Froude numbers yielded flows which were qualitatively the same as for small Mach numbers. For large Froude numbers, the shear component increased with Mach number, and the streamline displacement was more abrupt at higher Mach numbers.

The flow in a rotor-tip combustor of a helicopter ram jet was considered as an example, and the flow was shown to be appreciably affected by the action of a transverse body force.

Lewis Flight Propulsion Laboratory
National Advisory Committee for Aeronautics
Cleveland, Ohio, November 10, 1955

APPENDIX - SYMBOLS

The following symbols are used in this report:

B_{mn}	constants defined by eqs. (25)
C_{mn}	constants defined by eqs. (50)
c_p	specific heat at constant pressure
c_v	specific heat at constant volume
D	velocity difference between bottom and top of channel for uniform flow
Fr	Froude number, $U_\infty/\sqrt{(-f_2)H}$
f_i	i^{th} component of body force per unit mass, i = 1,2,3
H	channel height
h	function defined by eq. (18b)
L	channel width
M	Mach number, $U/\sqrt{\gamma RT}$
P	pressure
Q	rate of heat addition by sources per unit volume
Q_n	constants defined by eq. (22)
$\tilde{Q}$	constant defined by eq. (32)
q,q*	dimensionless heat parameters
R	gas constant
r	rotor radius
T	temperature
U,U_i,V,W	velocity components, i = 1,2,3
u,v,w	dimensionless perturbation velocity components

X, X_i, Y, Z dimensionless coordinates, $i = 1,2,3$

x, y, z dimensionless coordinates

$1(x)$ unit step function, $\int_{-\infty}^{x} \delta(x)dx = 1$ for $x > 0$, $= 0$ for $x < 0$

α length ratio, H/L

β $\sqrt{1 - M_\infty^2}$

Γ circulation

γ ratio of specific heats

$\delta(x)$ Dirac delta function, $\begin{cases} 0 & x \neq 0 \\ \infty & x = 0 \end{cases}$, $\int_{0^-}^{0^+} \delta(x)dx = 1$

ε small parameter (see eq. (4))

λ dimensionless parameter, $1/Fr^2 = (-f_2)H/U_\infty^2$

ξ, η, ζ transformed dimensionless coordinates

ρ density

σ dimensionless perturbation pressure

τ dimensionless perturbation temperature

φ potential function

$\bar{\varphi}$ potential function defined by eq. (46)

φ_i potential functions defined by eqs. (17), (18a), (19), and (20) $i = 1,2,3,4$

$\varphi^{(i)}$ potential functions defined by eq. (36)

χ dimensionless perturbation density

ψ density perturbation function defined by eq. (10)

$\psi^{(i)}$ density perturbation functions defined by eq. (36)

$\Omega_x, \Omega_y, \Omega_z$ dimensionless vorticity components

Subscripts:

r reference condition

T tip

∞ upstream condition

REFERENCE

1. Ostrach, Simon: Combined Natural- and Forced-Convection Laminar Flow and Heat Transfer of Fluids with and without Heat Sources in Channels with Linearly Varying Wall Temperatures. NACA TN 3141, 1954.

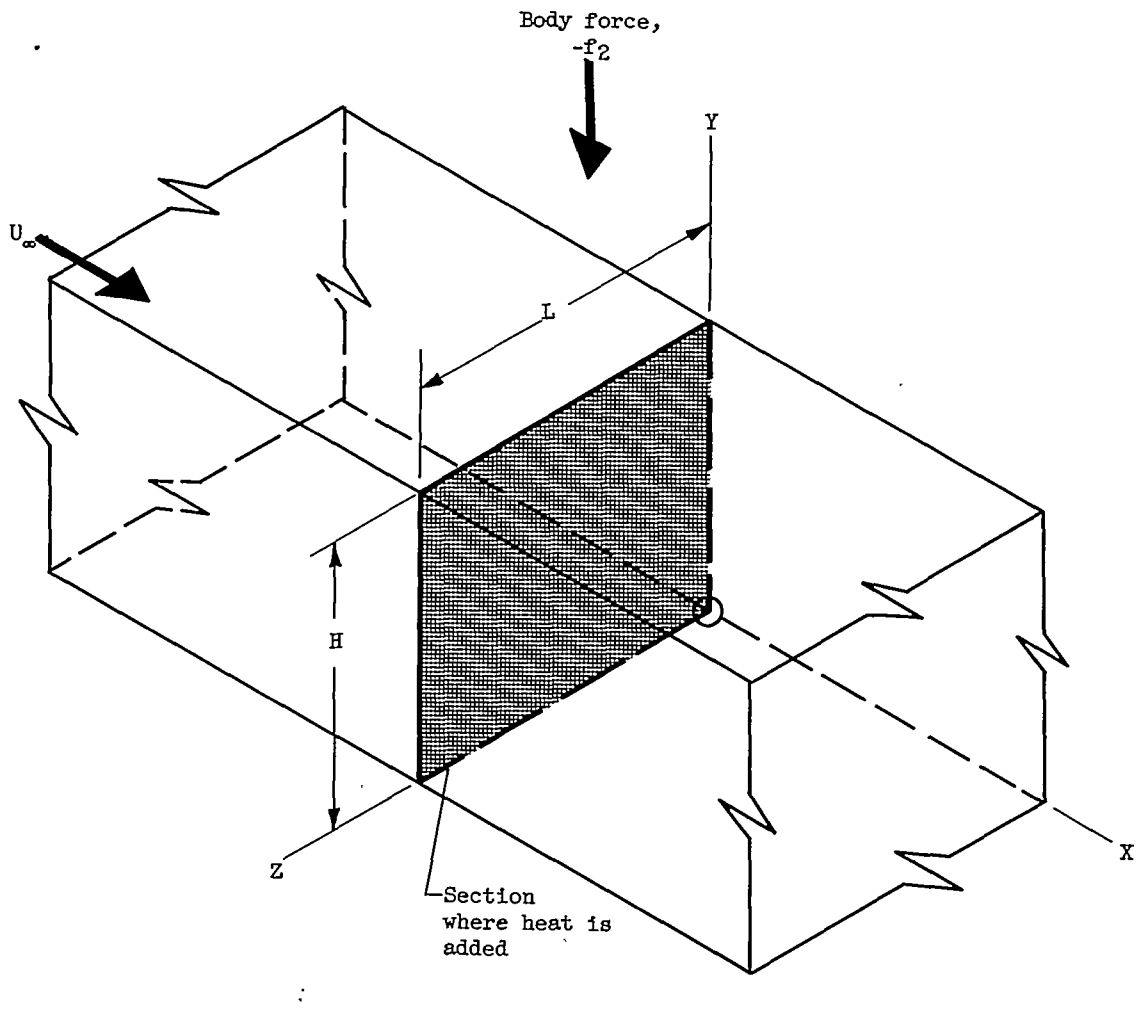

Figure 1. - Flow through a straight infinite channel with heat added at a cross-sectional plane, under transverse body force.

(a) Uniform heat addition; $q^* = Q_0$.

(b) Nonuniform heat addition; $q^* = \frac{\pi Q_0}{2}(1 - \cos 2\pi\alpha z)$.

Figure 2. - Cross-sectional pattern of heat addition at $x = 0$. Dark areas represent heat sources.

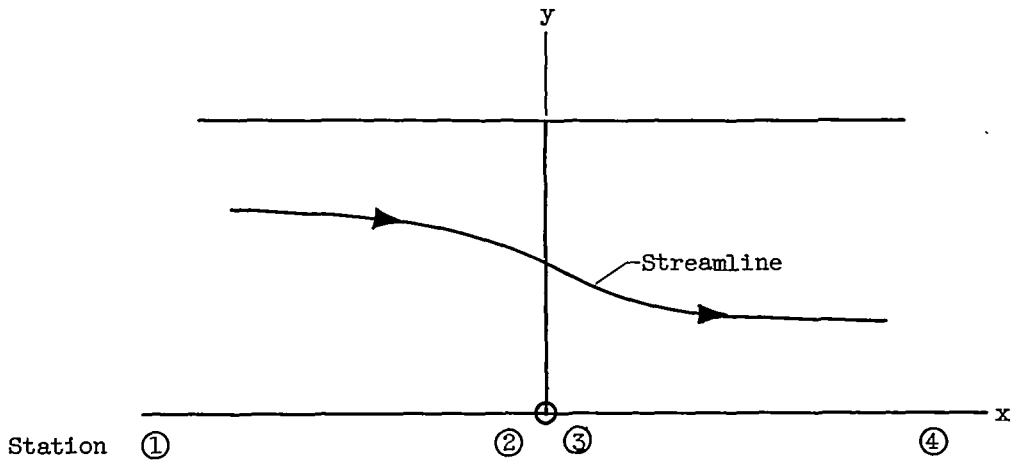

(a) Path of typical streamline in center of channel; side view.

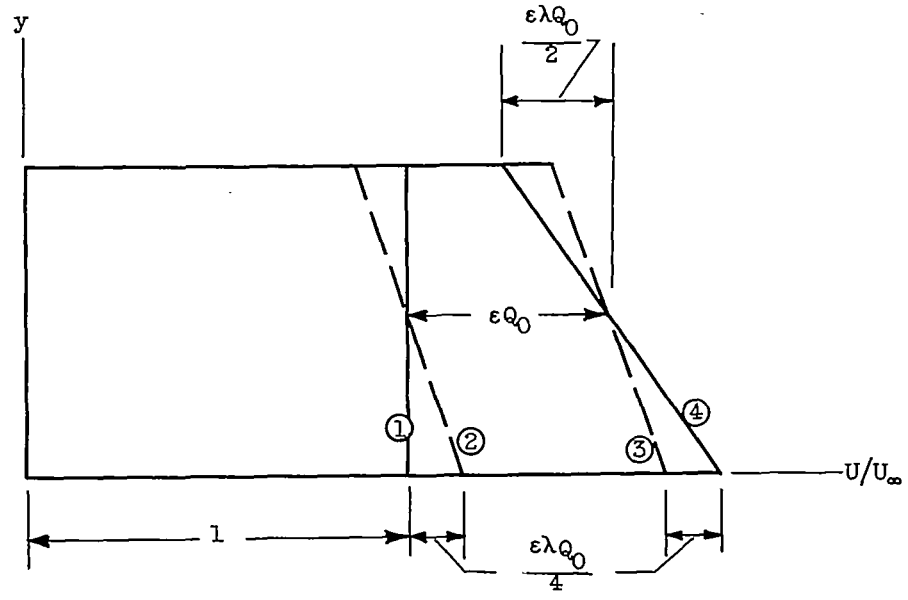

(b) Profiles of velocity.

Figure 3. - Results for heat added uniformly at plane x = 0 in two-dimensional channel. Station 1, far upstream; station 2, just upstream; station 3, just downstream; and station 4, far downstream.

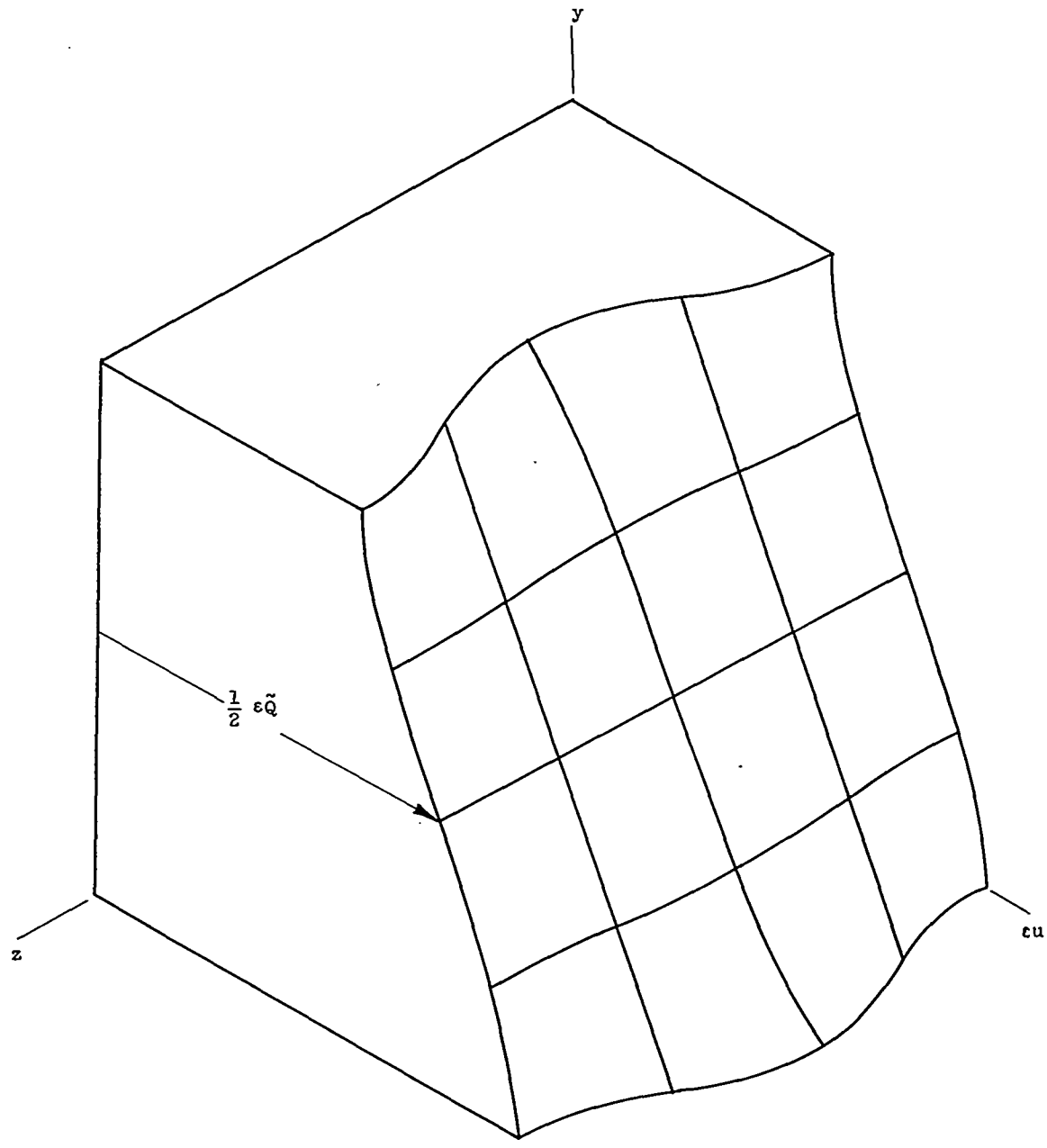

Figure 4. - Profile of increment in through velocity at large x for nonuniform heat addition. Mach number very much less than 1; length ratio, 1.

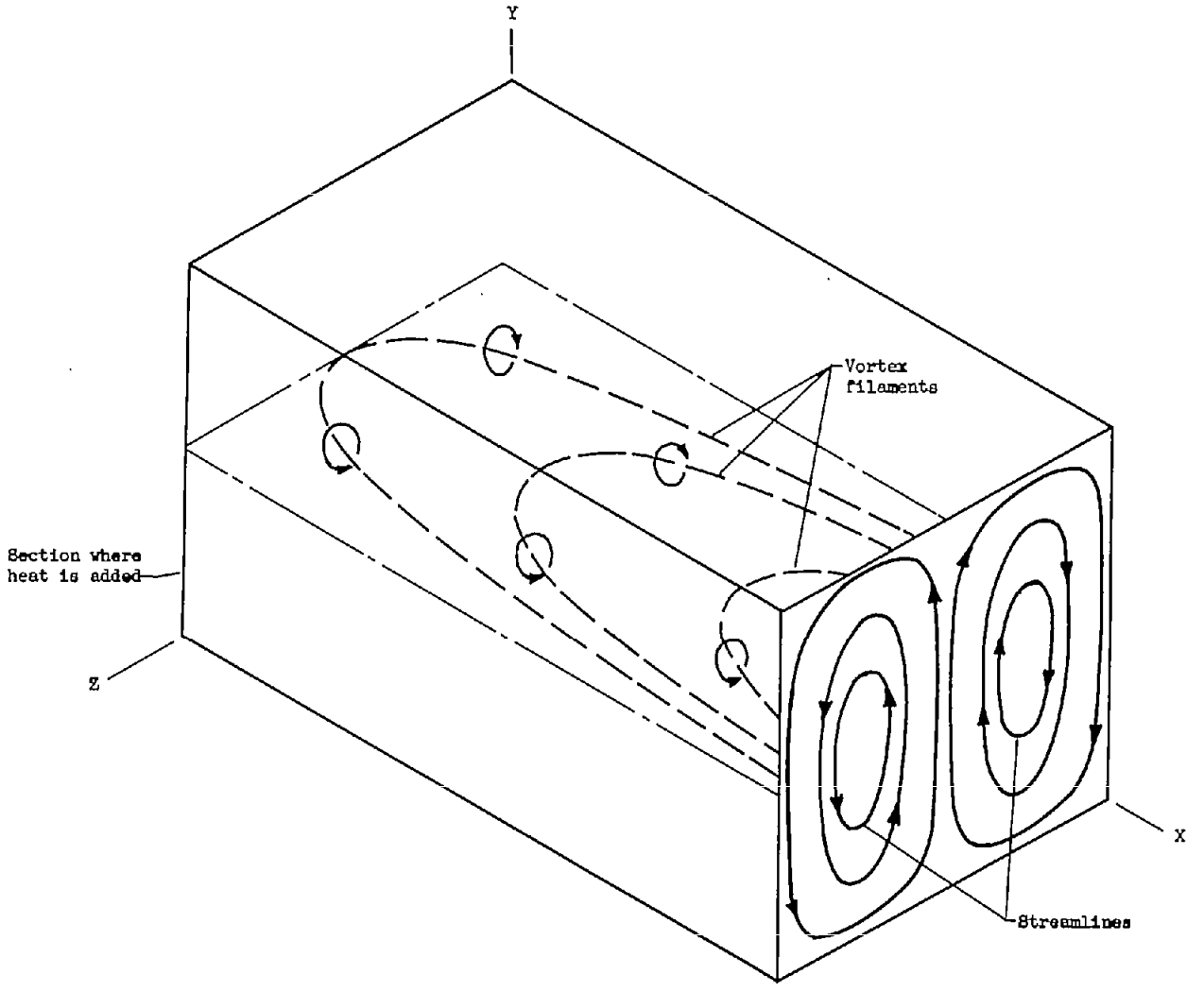

Figure 5. - Vortex filaments and associated streamline pattern generated by nonuniform heat addition. Mach number very much less than 1; length ratio, 1.